

Building of short circuit ampere - second characteristics for a series of amorphous core transformers

Bao Doan Thanh^{1*}

¹Faculty of Engineering & Technology Quy Nhon University

*Corresponding author E-mail: doanthanhbao@qnu.edu.vn

Abstract

This paper presents the development of a finite element method using Ansys Maxwell software to simulate the electromagnetic parameters of amorphous core transformers under three-phase short-circuit fault conditions on the low-voltage winding. The study calculates the maximum short-circuit current for both the low-voltage and high-voltage windings of each amorphous core transformers. Based on these findings, the short-circuit ampere-second characteristic of the amorphous core transformers is established, allowing operators to determine the optimal short-circuit disconnection time. This idea aids in the proper selection of fuse cutouts, preventing potential damage to transformer windings caused by harmful electromagnetic forces. Ultimately, this research helps protect transformers from winding displacement and failure due to short-circuit electromagnetic forces by ensuring timely activation of fuse cutouts and disconnection from the high-voltage system.

Keywords: Finite element method, Short-circuit current, Amorphous, Transformer, Ampere-second

1. Introduction

Amorphous core transformers (AMCTs) offer a significant advantage in reducing no-load loss by up to 70%. This is due to their unique composition and microstructure, which feature low coercive force, extremely thin steel sheets, and high resistivity. As a result, when used as the magnetic circuit in a transformer, the no-load loss is substantially lower compared to transformers with high-quality silicon steel core [1-3]. When the AMCTs is operating in no-load and rated modes, the interaction between current and magnetic fields (MFs) is minimal, resulting in small electromagnetic forces (EMFs) on the windings due to the relatively weak MFs. However, during a short-circuit (SC), the current in the winding increases and the MFs becomes much larger, generating a significant EMFs that acts on the windings. This force can produce mechanical stress that bends or damages the AMCTs windings [4, 5]. Winding failures account for 33% of all AMCTs failures, with these failures typically caused by SC between turns of the low voltage winding (LVW) and high voltage winding (HVW), between wire layers, between the LVW and HVW, or between phases within the same winding. These conditions create mechanical forces that can bend or destroy the AMCTs windings [6-8]. Figure 1 shows an actual AMCTs winding failure resulting from a SC. In [9], this paper employs simulink to construct a simulation model of inrush current. The inrush current characteristics of the converter transformer is then examined with different remanence and closing phase. Additionally, a finite element simulation model is created to investigate the iron core's saturation characteristics. In [10], the combination of the FEM and analytical model is developed for three-phase power transformer of a 50.000 kVA- 110 kV. The effect of SC impedance was evaluated in relation to the accumulated EMFs. Additionally, study on short-circuit current (SCC) was applied to this model to test the EMFs acting upon on the transformer windings. In [11], the fractional order characteristics of inductance and capacitance are taken into account, and a refined lumped parameter

equivalent circuit model of the windings is utilized. The paper evaluates the EMFs in the event of a phase-to-phase SC and contrasts it with the traditional integer order model. The findings indicate that this new approach yields a more precise calculation of EMFs, thus providing more accurate benchmarks for assessing the condition of the transformer.

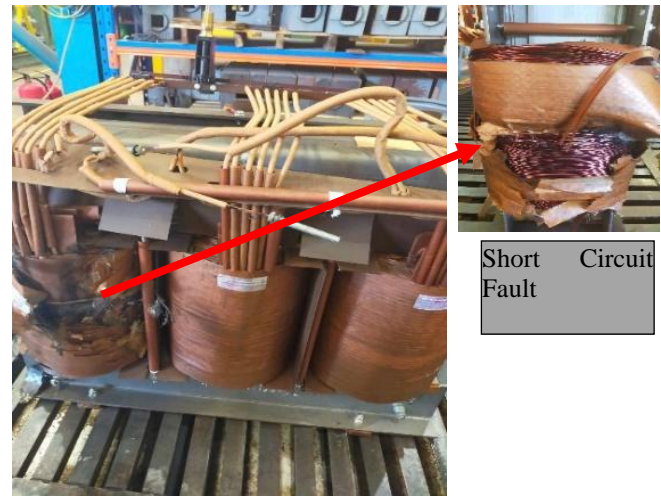


Figure 1. SC fault of AMCTs

In [12-17], the authors utilized FEM to analyze and calculate the allocation of dissipated MFs, reactive impedance, and EMFs acting on the HVW and LVW of the transformer during a SC. These studies also provided formulas for calculating currents and transient EMFs in SC conditions. The results of the average MFs density and EMFs, which were then compared with those obtained from classical analysis methods.

In this paper, a comprehensive analysis and evaluation of SC scenarios of the AMCTs is presented. An accurate model is first developed to properly assess the peak current value influencing with the MFs. The FEM is then proposed to simulate and validate the electromagnetic parameters of the practical AMCTs. To address this gap, this paper presents a model that achieves several valuable results. The study analyzes a series of AMCTs to determine the SCC values. From

these findings, a general SC ampere-second characteristic is developed. The results of this study are beneficial for transformer winding production, assisting operators in determining the optimal SC disconnection time and selecting the appropriate fuse cut-out (FCO) to protect the AMCTs from the damaging effects of SC EMFs that could compromise the windings.

2. Analytical method

2.1. Analytic model for computing leakage magnetic fields

The Laplace-Poisson's equation for $A(x,y,z)$ is expressed via the Maxwell's equations [1, 3, 5, 7]:

$$\nabla^2 \mathbf{A}(x, y, z) = \begin{cases} -\mu \mathbf{J} & \text{in the windings} \\ 0 & \text{others} \end{cases} \quad (1)$$

In 3D, the equation (1) can be written as:

$$\frac{\partial^2 \mathbf{A}(x, y, z)}{\partial x^2} + \frac{\partial^2 \mathbf{A}(x, y, z)}{\partial y^2} + \frac{\partial^2 \mathbf{A}(x, y, z)}{\partial z^2} = -\mu \mathbf{J} \quad (2)$$

where $\mathbf{A}(x,y,z)$ is the magnetic vector potential, μ is the relative permeability (H/m) and \mathbf{J} is the electric current (A/m²).

The MF density (\mathbf{B}) can be given as $\mathbf{B} = \nabla \times \mathbf{A}$, the components of \mathbf{B} in the x- and y- axis at the boundaries of the magnetic window are expressed as:

$$\begin{cases} B_x = \frac{\partial \mathbf{A}(x, y)}{\partial y} \\ B_y = -\frac{\partial \mathbf{A}(x, y)}{\partial x} \end{cases} \quad (3)$$

2.2. Short-circuit current

In case the transformer is working with the nominal primary voltage, if a SC occurs on the secondary side, the SCC will be very large. At this time, the entire nominal voltage is applied to the very small SC impedance of the transformer, so it is called an operating SC. The SCC is given as [1, 6, 17]:

$$\begin{aligned} i_{SC} &= i_{hos} + i_{dos} \\ &= I_{SC} \sqrt{2} \cdot \sin(\omega t - \phi - \varphi_{SC}) + I_{SC} \sqrt{2} \cdot \sin(\phi + \varphi_{SC}) \cdot e^{-\frac{R_{SC} \text{ot}}{X_{SC}}} \end{aligned} \quad (4)$$

Where:

i_{hos} is the harmonic oscillation;

i_{dos} is the damped oscillation;

ω is the angular frequency (rad/s);

ϕ is angle at the moment of SC (rad);

t is the time (s);

$I_{SC} = \frac{U_{Nominal}}{Z_{SC}}$ is the SC current (A) (where $U_{Nominal}$ is nominal voltage and Z_{SC} is the SC impedance (Ω));

$\varphi_{SC} = \arctg \frac{X_{SC}}{R_{SC}}$ is the phase angle (rad) (where R_{SC} is the resistance and X_{SC} is the reactance (Ω));

3. Finite element method

3.1. Three-phase AMCT 250kVA-22/0.4kV

An actual AMCTs with a capacity of 250kVA is pointed out in Figure 2. Table 2 presents the detailed electrical parameters of the AMCTs, and the entire simulation process in this study is based on the design drawings provided by the manufacturer in Hanoi, Vietnam.



Figure 2. AMCT of 250kVA

Figure 3 presents the meshing results for the machine, created using tetrahedral elements and analyzed within the Maxwell 3D environment. To improve the analysis efficiency, it is crucial to minimize the computational time. In this model, the insulation material and supporting structure have been omitted. Additionally, the concentric arrangement of the windings has been included in the Maxwell 3D model.

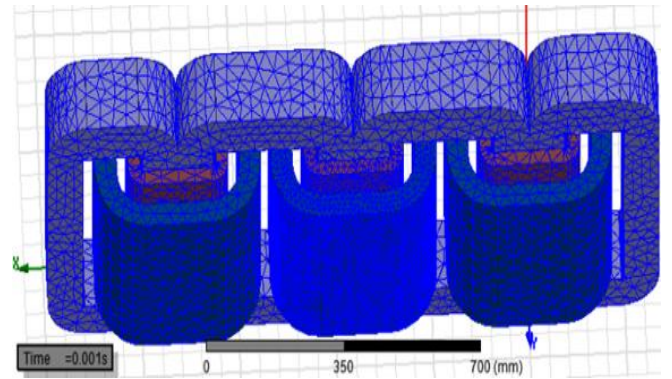


Figure 3. 3D-Mesh of the AMCTs 250kVA.

This test is analyzed in the time domain, with the analysis duration set to 0.2 seconds and a time step of 0.0001 seconds. Based on these parameters, the results show the distribution of magnetic inductance across the magnetic circuit and windings throughout the entire operating period of the AMCTs.

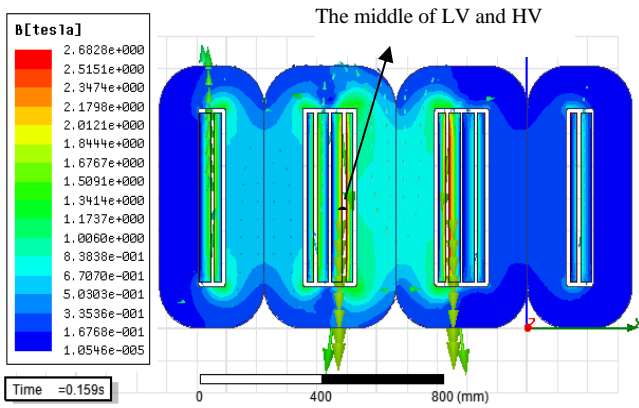


Figure 4. Distribution of MFs density with SCC.

As shown in Figure 4, at time $t = 59$ ms (when the SC on phase B attains its peak value), the MFs leakage in the winding area increases to $B = 2.68$ T, while the MFs in the core decreases. At this moment, the MFs leakage is most converging in the middle of the LVW and HVW. The SC fault on the upper LVW is controlled by the SC switch. The switch is closed to initiate the SC at 50 ms, as this is when the voltage of phase B is 0, and the SCC reaches its maximum value.

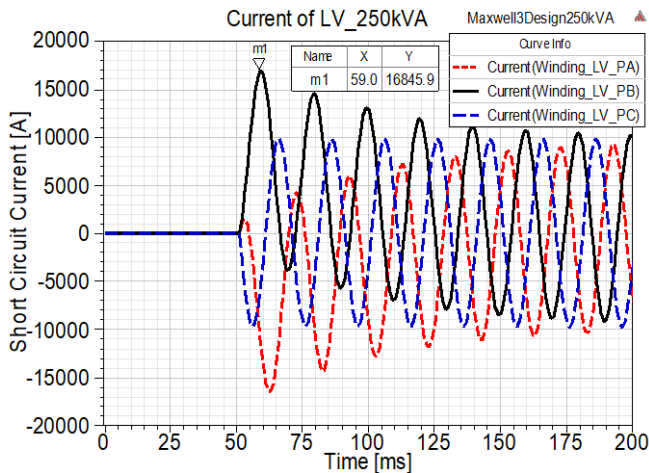


Figure 5. SCC in the LVW.

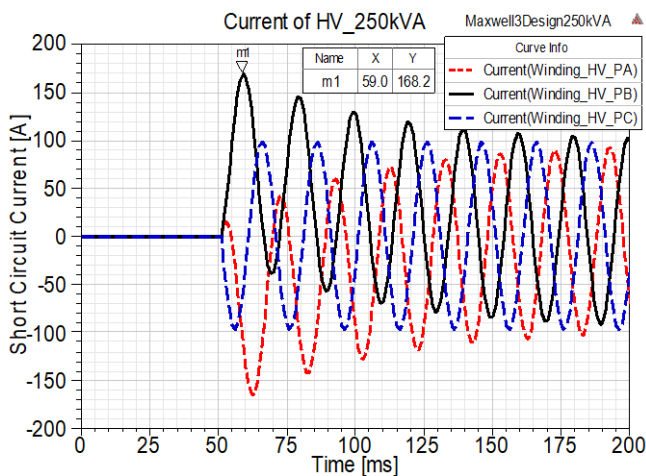


Figure 6. SCC in the HVW

The results of the SCC analysis for the LVW and HVW are shown in Figure 5 and Figure 6. At $t = 59$ ms, the peak

maximum SCC is: $I_{LV_max} = 16,845.9$ A for the LVW (phase B) and $I_{HV_max} = 168.2$ A for the HVW. These values are up to 33 times greater than the peak rated current. The corresponding values are summarized in Table 1.

Table 1. Maximum values on HVW and LVW

Windings	Peak rated current (A)	Peak Maximum SCC (A)	Ratio
LVW	$360.84\sqrt{2}$	16845.9	33
HVW	$3.79\sqrt{2}$	168.2	31.4

3.2. Simulation of AMSTs with varying power ratings

The FEM is used to simulate multiple transformers with varying capacities. We simulate ten transformers with different power ratings. As shown in Table 2, all transformers have a voltage rating of 22/0.4 kV and utilize Δ/Y wiring.

Table 2. Basic parameters of a three - phase AMTC

No.	Power (kVA)	Number of turns per phase in HV/LV (turns)	Nominal phase currents HVW/LVW (A)	No load $i_0\%$	voltage $u_k\%$
1	50	4002/40	0.76/72.17	0.8	4.2
2	100	3001/30	1.51/144.34	0.7	4.3
3	160	2802/28	2.42/231	0.6	4.17
4	250	2603/26	3.79/360.84	0.55	4.4
5	400	2001/20	6.06/577.4	0.53	4.4
6	630	1715/18	9.55/909.33	0.52	5.7
7	750	1605/16	11.36/1082.53	0.51	5.65
8	1000	1400/14	15.15/1443.4	0.50	5.6
9	1250	1305/13	18.94/1804.22	0.50	5.62
10	1600	1001/10	24.24/2309.4	0.50	5.6

3.2.1. Short-circuit currents of AMCTs 50kVA

In the same way, the FEM applied to the AMCTs of 50 kVA is simulated under three-phase SC conditions and analyzed using the Maxwell 3D environment.

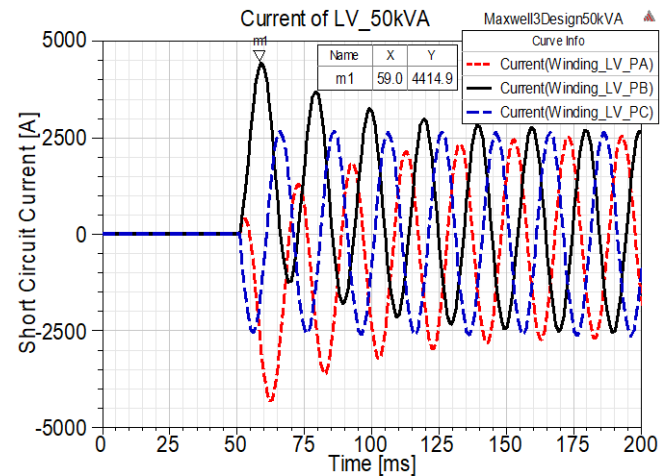


Figure 7. SCC in the LVW of AMCTs 50kVA.

The results of the SCC analysis for the LVW and HVW are presented in Figure 7 and Figure 8. At $t = 59$ ms, the peak

maximum SCC is: $I_{LV_max} = 4,414.9$ A for the LVW (phase B) and $I_{HV_max} = 44.1$ A for the HVW. These values are up to 43 times greater than the peak rated current.

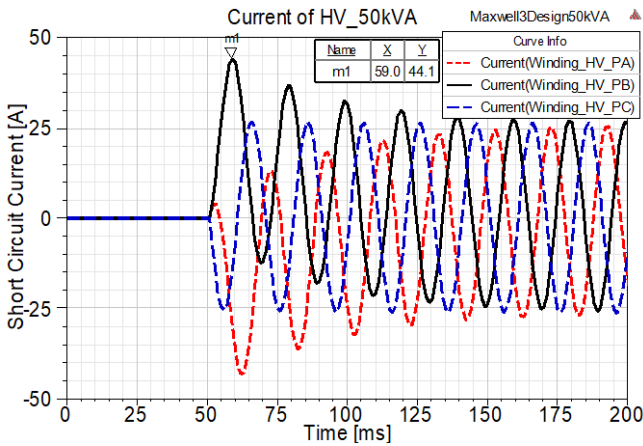


Figure 8. SCC in the HVW of AMCTs 50kVA.

3.2.2. Short-circuit currents of AMCTs 750kVA

In this section, the AMCTs of 750kVA is simulated for three-phase SC condition and analyzed in Maxwell 3D analysis.

The results of the LVW and HVW under the SCC analysis are shown in Figure 9 and Figure 10. It can be seen that at $t = 59$ ms, the peak value of the maximum SCC on LVW phase B, $I_{LV_max} = 43131.5$ A and $I_{HV_max} = 429.9$ A for the HVW. This means that it is as much as 28 times higher.

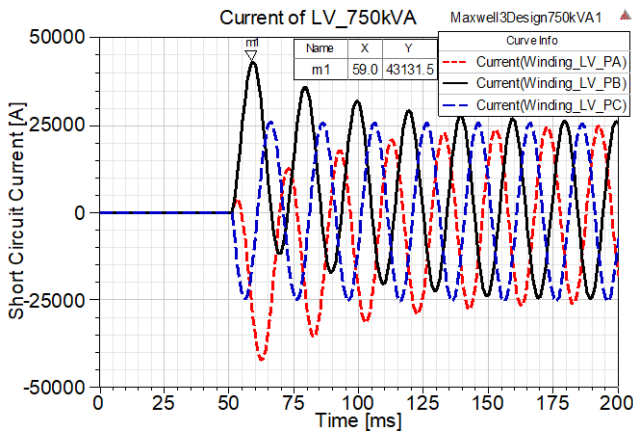


Figure 9. SCC in the LVW of AMCTs 750kVA

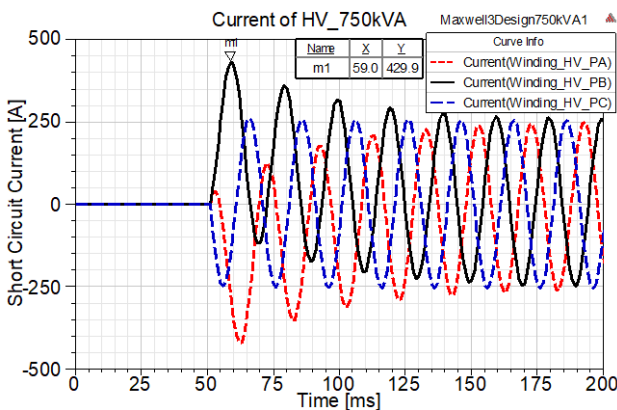


Figure 10. SCC in the HVW of AMCTs 750kVA

3.2.3. Short-circuit currents of AMCTs 1250kVA

The 1250 kVA AMCTs is simulated under three-phase SC conditions and analyzed using the Maxwell 3D environment.

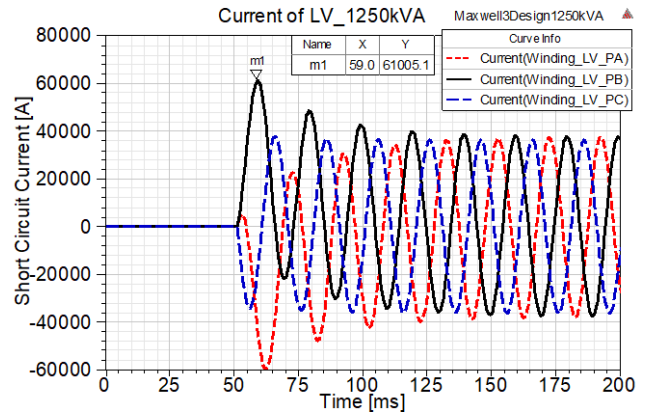


Figure 11. SCC in the LVW of AMCTs 1250kVA

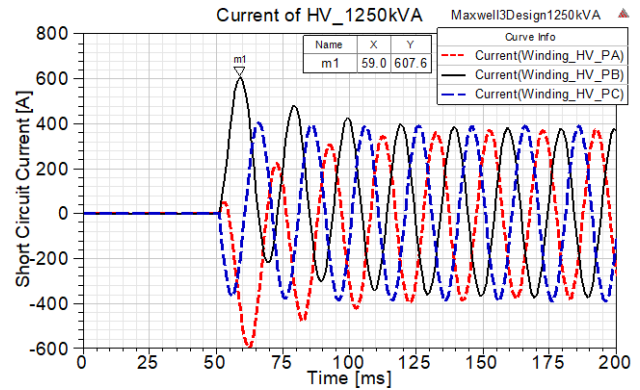


Figure 12. SCC in the HVW of AMCTs 1250kVA

The results of the SCC analysis for the LVW and HVW are shown in Figure 11 and Figure 12. At $t = 59$ ms, the peak maximum SCC is: $I_{LV_max} = 61,005.1$ A for the LVW (phase B) and $I_{HV_max} = 607.6$ A for the HVW. These values are up to 32 times greater than the peak rated current.

3.2.4. Short-circuit currents of AMCTs 1600kVA

In this part, the AMCTs of 1600 kVA is also simulated under the three-phase SC conditions and analyzed using the Maxwell 3D environment.

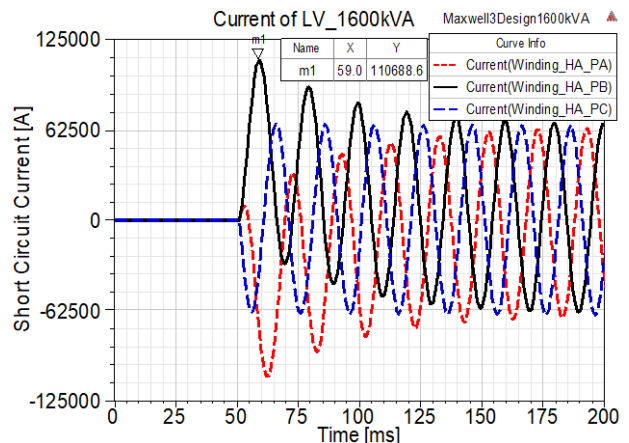


Figure 13. SCC in the LVW of AMCTs 1600kVA

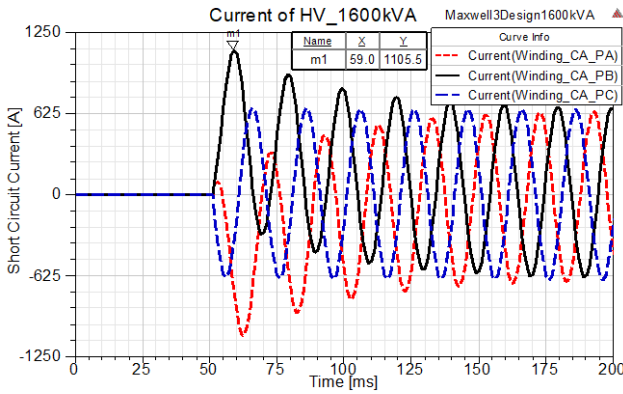


Figure 14. SCC in the LVW of AMCTs 1600kVA

The results of the SCC analysis for the LVW and HVW are shown in Figure 13 and Figure 14. At $t = 59$ ms, the peak maximum SCC is: $I_{LV_max} = 110,688.6$ A for the LVW (phase B) and $I_{HV_max} = 1,105.5$ A for the HVW. These values are up to 32 times greater than the peak rated current.

4. Resultant of ten AMCTs

4.1. Resultant of short-circuit currents

The SCC were simulated for the LVW and HVW of AMCTs with power ratings ranging from $S = 50$ to 1600 kVA. The results from the 10 cases are presented in Table 3.

Table 3. Resultant of SCC

No.	Power (kVA)	SCC on windings (A)	
		LVW	HVW
1	50	4414.9	44.1
2	100	6797.4	87.7
3	160	10 397	118,7
4	250	16845.9	168.2
5	400	22663.2	226.5
6	630	29066.8	305.1
7	750	43131.5	429.9
8	1000	54448.3	544.4
9	1250	61005.1	607.6
10	1600	110688.6	1105.5

The SCC results presented in Table 3 are represented graphically for the ten AMCTs in Figure 15.

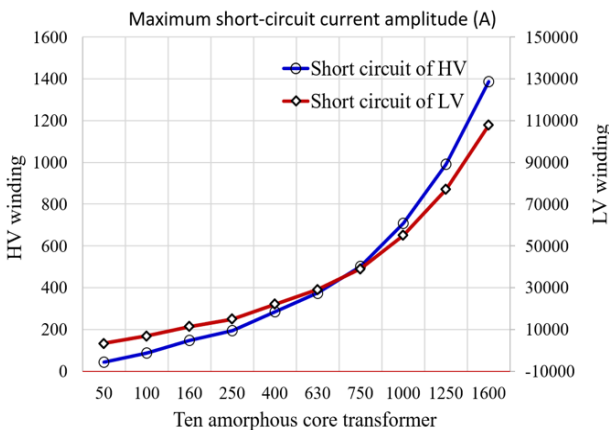


Figure 15. SCC of ten AMCTs

As shown in Figure 15, the SCC results for the LVW and HVW are presented for each transformer power rating.

4.2. Building of short-circuit Ampere - second (A.s) characteristics

The AMCTs is operating with the HVW, which is protected by the FCO, while the LVW experiences a simultaneous three-phase SC. The FCO (denoted as K) is used to protect the HVW from large overloads and SC in distribution transformers [18]. Using the SCC values for the HVW of the ten AMCTs from Table 3, we have constructed the Ampere-second (A.s) graph for these 10 transformers, as shown in Figure 16.

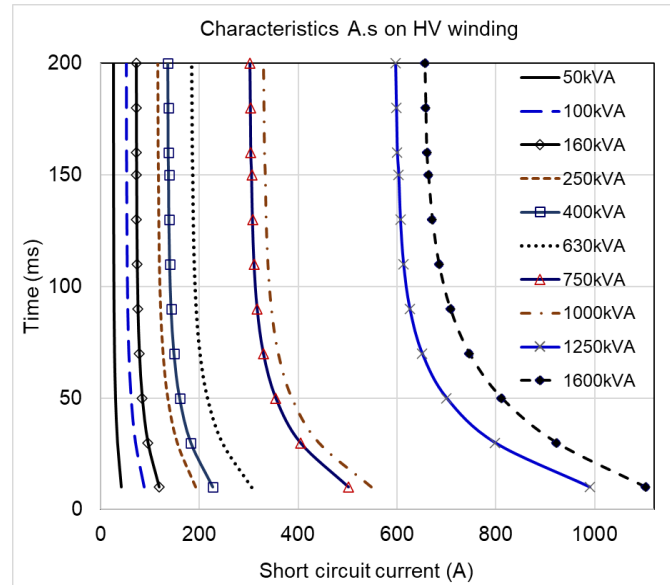


Figure 16. SC Ampere – second (A.s) characteristics on HVW of ten AMCTs.

In practice, the FCOs are used to protect distribution transformers from large overloads and SC. By referring to the SC Ampere-second (A.s) characteristics of the ten transformers shown in Figure 16, transformer operators can determine the optimal SC disconnection time, allowing them to select the most appropriate fuse wire for the FCO.

5. Conclusion

This paper uses the FEM with Ansys Maxwell software to emulate the operational modes of AMCTs with power ratings ranging from 50 kVA to 1600 kVA and a voltage of 22/0.4 kV. The SCC results are compared with preliminary calculations. The research finds that the maximum SCC in the HVW and LVW can be up to 43 times higher than the rated phase current. The key contributions of this study are: (1) developing the characteristics of the peak value SCC for both LVW and HVW across various transformer power ratings, and (2) establishing the relationship between SCC and time. The SC ampere-second (A.s) characteristics for ten AMCTs are provided, helping transformer operators select the most appropriate FCO for SC protection. The findings of this research assist operating engineers and AMCTs manufacturers in determining the correct FCO SC time to disconnect the AMCTs from the high-voltage grid. This research will expand knowledge in

the future, first by establishing the relationship between the EMFs from the SC and the winding radius, and second by identifying the area where winding destruction is limited according to transformer power ratings.

References

- [1] B. D. Thanh, C. P. Do, H. D. Hoan and L. T. Hiep, "Analysis of Current and Electromagnetic Force Acting on Winding in Cases of Short Circuits of Amorphous Transformer," *2023 8th International Scientific Conference on Applying New Technology in Green Buildings (ATiGB)*, Danang, Vietnam, 2023, pp. 201-208.
<https://doi.org/10.1109/ATiGB59969.2023.10364484>.
- [2] T. Bao Doan and C. Phi Do, "Calculation of the Magnetic Field and Inrush Current in a Three-phase Transformer," *2020 Applying New Technology in Green Buildings (ATiGB)*, Da Nang, Vietnam, 2021, pp. 94-99.
<https://doi.org/10.1109/ATiGB50996.2021.9423111>.
- [3] Y. Zhao *et al.*, "Short-Circuit Electromagnetic Force Distribution Characteristics in Transformer Winding Transposition Structures," in *IEEE Transactions on Magnetics*, vol. 56, no. 12, pp. 1-8, Dec. 2020, Art no. 8400708.
<https://doi.org/10.1109/TMAG.2020.3028832>
- [4] K. Dawood and G. Komurgoz, "Investigating effect of Electromagnetic Force on Sandwich Winding Transformer using Finite Element Analysis," *2021 28th International Workshop on Electric Drives: Improving Reliability of Electric Drives (IWED)*, Moscow, Russia, 2021, pp. 1-5.
<https://doi.org/10.1109/IWED52055.2021.9376371>
- [5] Deren Li, Liang Zhang, Guangmin Li, Zhichao Lu Shaoxiong Zhou (2012) *Reducing the core loss of amorphous cores for distribution transformers*. Prog. Nat. Sci. Mater. Int., vol. 22, no. 3, p. 244-249.
- [6] Hajiaghahi Salman, Karim Abbaszadeh (2013) *Analysis of Electromagnetic Forces in Distribution Transformers Under Various Internal Short-Circuit Faults*. CIRED Reg. - Iran, Tehran, vol. 13-14, p. 1-9.
- [7] C. -H. Hsu, C. -Y. Lee, Y. -H. Chang, F. -J. Lin, C. -M. Fu and J. -G. Lin, "Effect of Magnetostriction on the Core Loss, Noise, and Vibration of Fluxgate Sensor Composed of Amorphous Materials," in *IEEE Transactions on Magnetics*, vol. 49, no. 7, pp. 3862-3865, July 2013.
<https://doi.org/10.1109/TMAG.2013.2248702>
- [8] Y. Li, Q. Xu and Y. Lu, "Electromagnetic Force Analysis of a Power Transformer Under the Short-Circuit Condition," in *IEEE Transactions on Applied Superconductivity*, vol. 31, no. 8, pp. 1-3, Nov. 2021, Art no. 0603803.
<https://doi.org/10.1109/TASC.2021.3107799>.
- [9] Y. Yu, Z. Zhanlong, H. Wenhao, C. Junxin and L. Dingyuan, "Simulation Analysis of Inrush Current and Electromagnetic-Force Characteristics of Converter Transformer During No-Load Closing," *2023 2nd International Conference on Power Systems and Electrical Technology (PSET)*, Milan, Italy, pp. 137-143, 2023.
<http://doi.org/10.1109/PSET59452.2023.10346443>
- [10] M. Jin *et al.*, "Influence of Frequency Components of Short-Circuit Electromagnetic Force on Vibration Characteristics of Power Transformer Windings," *2022 IEEE International Conference on High Voltage Engineering and Applications (ICHVE)*, Chongqing, China, 2022, pp. 01-04.
<https://doi.org/10.1109/ICHVE53725.2022.9961671>.
- [11] Y. Song, Y. Lu, L. Zhang *et al.*, "Electromagnetic Force Analysis of Short-circuit Faults in Transformer Windings Based on Fractional-order Models," *2024 3rd Asian Conference on Frontiers of Power and Energy (ACFPE)*, Chengdu, China, pp. 514-520, 2024.
<https://doi.org/10.1109/ACFPE63443.2024.10800964>
- [12] M. Nazmunnahar, S. Simizu, P. R. Ohodnicki, S. Bhattacharya and M. E. McHenry, "Finite-Element Analysis Modeling of High-Frequency Single-Phase Transformers Enabled by Metal Amorphous Nanocomposites and Calculation of Leakage Inductance for Different Winding Topologies," in *IEEE Transactions on Magnetics*, vol. 55, no. 7, pp. 1-11, July 2019, Art no. 8401511.
<https://doi.org/10.1109/TMAG.2019.2904007>
- [13] L. Roginskaya, Z. Yalalova, A. Gorbunov and J. Rakhmanova, "Features of amorphous steel magnetic cores for transformers operating at mains frequency," *2020 International Conference on Electrotechnical Complexes and Systems (ICOECS)*, Ufa, Russia, 2020, pp. 1-5.
<https://doi.org/10.1109/ICOECS50468.2020.9278451>
- [14] Sharifan M. B. B., R. Esmaeilzadeh, M. Farrokhifar, J. Faiz, M. Ghadimi, G. Ahrabian (2008) "Computation of a single-phase shell-type transformer windings forces caused by inrush and short-circuit currents," *J. Comput. Sci.*, vol. 4, no. 1, p. 51-58.
<https://doi.org/10.3844/jcssp.2008.51.58>
- [15] S. Bal, T. Demirdelen and M. Tümay, "Three-Phase Distribution Transformer Modeling and Electromagnetic Transient Analysis Using ANSYS Maxwell," *2019 3rd International Symposium on Multidisciplinary Studies and Innovative Technologies (ISMSIT)*, Ankara, Turkey, 2019, pp. 1-4.
<https://doi.org/10.1109/ISMSIT.2019.8932953>
- [16] Y. Zhai, R. Zhu, Q. Li, X. Wang, Y. Gu and S. Li, "Simulation Research on Electrodynamic Force and Deformation of Transformer Windings under Short-circuit Condition," *2022 IEEE International Conference on High Voltage Engineering and Applications (ICHVE)*, Chongqing, China, 2022, pp. 1-4
<https://doi.org/10.1109/ICHVE53725.2022.9961358>.
- [17] Y. Zhao, T. Wen, Y. Li, H. Ni, Q. Zhang and W. Chen, "A FEM-based simulation of electromagnetic forces on transformer windings under short-circuit," *2018 IEEE International Power Modulator and High Voltage Conference (IPMHVC)*, Jackson, WY, USA, 2018, pp. 425-429.
<https://doi.org/10.1109/IPMHVC.2018.8936726>.
- [18] Nguyễn Hoàng Việt (2005) *Bảo vệ role và Tự động hoá trong hệ thống điện*, NXB Đại học Quốc Gia Hồ Chí Minh, pp. 1-492.